J Mater Sci (2010) 45:1837–1845
DOI 10.1007/s10853-009-4167-3

Structure, electrical, and optical properties of ZnO-substituted PbO for the Er^{3+}/Yb^{3+} co-doped Bi_2O_3–GeO_2–Na_2O glass system

Shaaban M. Salem · I. Shaltout

Received: 27 July 2009 / Accepted: 24 December 2009 / Published online: 12 January 2010
© Springer Science+Business Media, LLC 2010

Abstract Glasses of the $0.5Er^{3+}/2.5Yb^{3+}$ co-doped (40 Bi_2O_3–$20GeO_2$–$(30 - x)$PbO–xZnO–$10Na_2O$ system where $x = 0.0$, 5, 10, 15, 20, 25, and 30 mol%) have been characterized by FT-IR spectroscopy measurements to obtain information about the influence of ZnO-substituted PbO on the local structure of the glass matrix. The density and the molar volume have been determined. The influences of the ZnO-substituted PbO on the structure of glasses have been discussed. The dc conductivity measured in the temperature range 475–700 K obeys Arrhenius law. The conductivity decreases while the activation energy for conduction increases with increase ZnO content. The optical transmittance and reflectance spectrum of the glasses have been recorded in the wavelength range 400–1100 nm. The values of the optical band gap E_{opt} for all types of electronic transitions and refractive index have been determined and discussed. The real and imaginary parts ε_1 and ε_2 of dielectric constant have been determined.

Introduction

It is well known that heavy metal oxide glasses (HMOG) based on PbO and Bi_2O_3 have interesting physical properties such as high density, high linear, and non-linear refractive index enabling their extensive various applications in optics and optoelectronics [1, 2]. Glasses with covalent networks often tend to possess open structures and support high ionic conductivities [3]. The investigation of the structure of such materials is essential to obtain a better insight into the structure–property relations. Despite the fact that Bi_2O_3 is not a classical glass former, due to high polarizability and small field strength of Bi^{3+} ions, in the presence of conventional glass formers (such as B_2O_3, PbO, SiO_2, etc.) it may build a glass network of $[BiO_n]$ ($n = 3$, 6) pyramids [4, 5]. However, the structural role played by Bi_2O_3 in glasses is complicated and poorly understood. This is because the $[BiO_n]$ polyhedra are highly distorted due to the lone pair electrons. Several techniques have been employed in an attempt to identify the local environment of the different elements in bismuthate glasses. The glass structure is also influenced by the presence of other constituents like ZnO and PbO, as these cations can enter the glass network both as network former and as network modifier [6].

With the development of upconversion visible or ultraviolet photonic devices, rare earth ions-doped glasses have been investigated extensively, which may be the candidate materials to be applied in areas of high-density optical storage, color displays, optoelectronics, and medical diagnostics [7]. The trivalent Er^{3+} ion has already established a key role as the active dopant for the optical amplification at $\sim$1.5 μm in the telecommunications window as well as for up-conversion-based lasers generating laser emissions at mid infrared and visible regions (at $\sim$2.8, $\sim$0.55, and $\sim$0.66 μm). However, the corresponding transitions have weak ground state absorption, notably at 980 nm. Hence, a sensitizer is indispensable for the achievement of high optical pumping efficiency [8]. Yb^{3+} seems to have the appropriate feature for this role since there is an important spectral overlap between its $^2F_{5/2} \rightarrow {}^2F_{7/2}$ emission band and the Er^{3+} $^4I_{15/2} \rightarrow {}^4I_{11/2}$ absorption band, allowing for an efficient $Yb^{3+} \rightarrow Er^{3+}$ transfer of the excitation energy. This fact, combined to a high Yb^{3+} absorption cross section at $\sim$ 980 nm, yields increasing luminescence efficiency in

S. M. Salem (✉) · I. Shaltout
Department of Physics, Faculty of Science, Al Azhar University, Nasr City, 11884 Cairo, Egypt
e-mail: shaabansalem@gmail.com

co-doped systems [9]. Among oxide glasses, bismuth glasses have been intensively investigated because of their special properties such as the possibility to incorporate a large amount rare-earth dopants, high refractive index and relative low phonon energy. Therefore, the present work has been carried out to investigate the influences of the ZnO-substituted PbO on the density, molar volume, structure, dc conductivity, and optical properties of the $0.5Er^{3+}/2.5Yb^{3+}$ co-doped $(40Bi_2O_3–20GeO_2–(30 - x)PbO–xZnO–10Na_2O$ system where $x = 0.0$, 5, 10, 15, 20, 25, and 30 mol%).

Experimental

Glass samples of compositions ($0.5Er^{3+}/2.5Yb^{3+}$ co-doped $40Bi_2O_3–20GeO_2–(30 - x)PbO–xZnO–10Na_2O$ system where $x = 0.0$, 5, 10, 15, 20, 25, and 30 mol%) were prepared by melt quench technique using reagent grade chemicals Bi_2O_3, ZnO, PbO, GeO_2, and Na_2CO_3. The mixture of these chemicals taken in porcelain crucibles and then melted at 1150 °C using electrical furnace for 1 h to ensure homogeneous mixture. The clear liquid (free of bubbles) was quickly cast in a copper mold kept at room temperature and pressed with another copper disk maintained at the same temperature, the obtained glass samples were transparent. The obtained glass was cut and polished carefully to meet the requirements for optical and electrical measurements. X-ray powder diffraction XRD measurements have been carried out on Shimadzu XD-DI, X-ray Diffractometer VG 207RII and $CuK_\alpha = 1.54056$ Å for grounded powder of the as-quenched samples as a necessary technique for proving the amorphous nature of the samples. The density of the samples measured at room temperature was measured by Archimedes principle using carbon tetrachloride as an immersion liquid. The molar volume (V_m), atomic concentration N, and atomic intermediate distance R were estimated. The dc electrical conductivity measured by means of two-probe method, which appropriate for high-resistance materials. Silver-painted electrodes were pasted on the polished surface of the samples then situated between two polished and cleaned copper electrodes. The current is monitored by means of an electrometer [model: 425A HP], milivoltmeter for measuring the temperature over temperature range (475–700 K) with constant voltage source 24 V and a home-made furnace.

Infrared spectra of the powdered glass samples were recorded at room temperature in the range 450–1500 cm^{-1} using a spectrometer (Perkin-Elmer FT-IS, model 1605). These measurements were made on glass powder dispersed in KBr pellets. The absorption spectra were recorded in the range of 190–1100 nm Jasco V-570 Spectrophotometer.

Results and discussion

Amorphous nature of all prepared samples was confirmed using X-ray diffraction. The density (ρ) of the glass samples determined in the present study is given in Table 1. The molar volume (V_m) of the glass samples was calculated using the molecular weight (M) and density (ρ) with the following relation:

$$V_m = M/\rho \quad (1)$$

The atomic concentration, N (cm^{-3}), was calculated using the formula $N = \rho N_A/M$, N_A is Avogadro's number, M is the molecular weight, and ρ is the density, and the atomic intermediate distance $R = (1/N)^{1/3}$.

The density and molar volume as a function of concentration of ZnO mol% are shown in Fig. 1. It is seen from Table 1 and Fig. 1 that the density decreases with increase in ZnO content. Since ZnO has molecular mass less than the molecular mass of PbO, therefore, it is an expected result. On the other hand, the increase in ZnO concentration density decreases significantly, which may be due to the strong influence of the packing density, which provides fairly open structure in the glass matrix. The variation of V_m with ZnO is shown in Fig. 1. It is observed that V_m increases with increase in ZnO content up to

Table 1 Chemical composition and physical properties of $0.5Er^{3+}/2.5Yb^{3+}$ co-doped $(40Bi_2O_3–20GeO_2–(30 - x)PbO–xZnO–10Na_2O$, where $x = 0$, 5, 10, 15, 20, 25, and 30 mol%) glasses

Glass no.	Composition (mol%)					d (g cm^{-3})	V_m (cm^3/mol)	$N \times 10^{22}$ (cm^{-3})	R (Å)	W (eV)
	Bi_2O_3	GeO_2	PbO	ZnO	Na_2O					
1	40	20	30	0.0	10	6.78	43.62	1.386	4.16	1.122
2	40	20	25	5.0	10	6.68	43.20	1.394	4.15	1.113
3	40	20	20	10	10	6.42	43.87	1.373	4.17	1.225
4	40	20	15	15	10	6.81	44.41	1.356	4.19	1.338
5	40	20	10	20	10	5.92	45.21	1.332	4.22	1.344
6	40	20	5.0	25	10	5.77	45.14	1.334	4.22	1.408
7	40	20	0.0	30	10	5.44	46.52	1.295	4.25	1.472

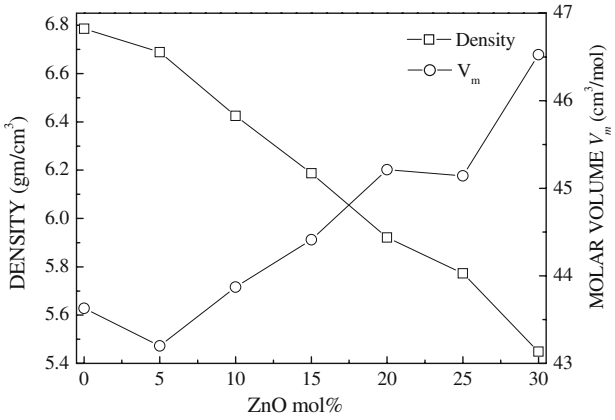

Fig. 1 The density d and molar volume V_m as a function of ZnO-substituted PbO for Er^{3+}/Yb^{3+} co-doped ($40Bi_2O_3$–$20GeO_2$–$(30 - x)$ PbO–xZnO–$10Na_2O$) glasses

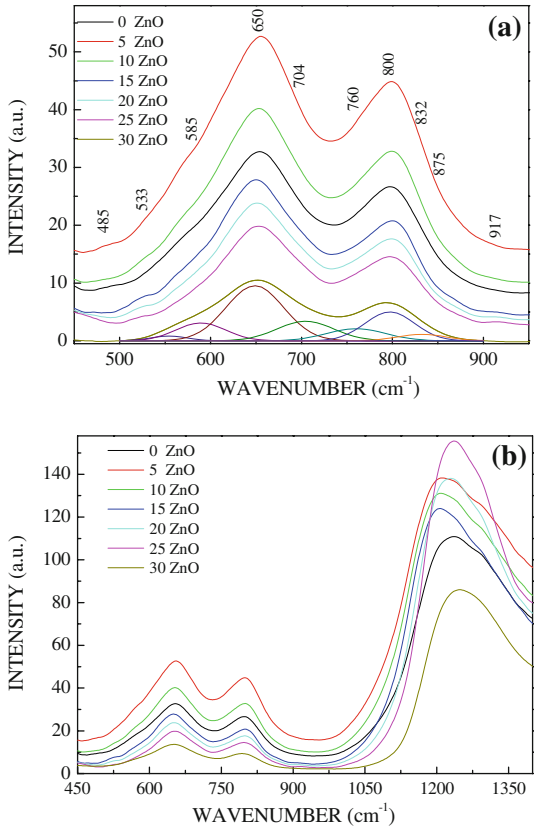

Fig. 2 IR absorption spectra of Er^{3+}/Yb^{3+} co-doped ($40Bi_2O_3$–$20GeO_2$–$(30 - x)$PbO–xZnO–$10Na_2O$) glasses in **a** the wavenumber region 450–1000 cm^{-1} and **b** 450–1350 cm^{-1}, respectively

30 mol%, which is attributed to, PbO enter the glass as network modifiers while ZnO enter the glass as network modifiers or as network formers [4–6]. Therefore, with increasing of ZnO at the expense of PbO content, the compactness of the network structure decrease and a corresponding increase of the molar volume (V_m).

The IR absorption spectra of the $0.5Er^{3+}/2.5Yb^{3+}$ co-doped ($40Bi_2O_3$–$20GeO_2$–$(30 - x)$PbO–xZnO–$10Na_2O$ system where $x = 0.0$, 5, 10, 15, 20, 25, and 30 mol%) glasses are shown in Fig. 2a and b. FT-IR spectroscopy was used to obtained essential information concerning the arrangement of the structural units of these glasses. The systematically changed IR spectra of the glasses under study showed the presence broad bands at ~ 485, 533, 602, 650, 704, 760, 800, 832, 875, 917, and 1236 cm^{-1} in the wave number range of 450–1450 cm^{-1}. The band at ~485 cm^{-1} which are due to the Bi–O bonds, bending vibrations in BiO_3 units [10], ~533 cm^{-1} which have been attributed to the Bi–O bending vibrations in BiO_6 units [11] and ~602 cm^{-1} that was ascribed to the Bi–O^-/Bi–O–Zn stretching vibration in the BiO_6 units [12]. The presence of IR band in the range 400–600 cm^{-1} indicates the presence of Zn–O tetrahedral bending vibrations in the present glass system [11]. It is clearly observed that with increase in the ZnO content the band 602 cm^{-1} increases in intensity which indicates the formation of the ZnO_4 units [11, 12]. The band at ~650 cm^{-1} which have been attributed to the interconnected germanium oxygen tetrahedral GeO_4 with non-bridging oxygen, modification of this network is manifested by the formation of GeO_6 germanium oxygen octahedra [13]. The bands at ~704 and 760 cm^{-1}, which are due to the Ge–O bonds vibrations in the GeO_4 units [14–16]. The band observed at ~832 cm^{-1} was assigned to Bi–O bonds vibrations in BiO_6 units [10, 17]. The bands from ~875 to 917 cm^{-1} were ascribed to Ge–O–Ge double degenerate stretching vibrations and Ge–O stretching vibrations in GeO_4 units [10].

The band around 797 cm^{-1}, for the prepared glass system was observed, due to the stretching vibrational modes of the glass network former. Pure GeO_2 glass has phonon bands around 860 cm^{-1}. The presence of PbO or/and ZnO in the glass system makes the Ge–O bond weaker, shifting its band to 797 cm^{-1} [18]. Similar Raman and IR spectra were measured for other Bi_2O_3–GeO_2 glasses reported in previous literature [13, 15]. The position of the band around 797 cm^{-1} is important because the multiphonon decay of rare-earth ions in a glass depends on this value in the host glass [19, 20]. The position of this band did not change for the different compositions.

The adding of ZnO in glass samples produces some change in the FT-IR spectrum. Thus, the band from ~832 cm^{-1} disappears and a new band situated at ~875 cm^{-1} is present in the samples containing 15, 20, 25, and 30 mol%. This suggests the conversion of the BiO_3 into BiO_6 structural units with the increasing of ZnO ions content in the glass samples. Thus, the presence of ZnO ions in the glass samples seems to influence the surrounding of the Bi^{3+} cations favoring the formation of the BiO_6 units. The band at ~485 cm^{-1} shift to lower wavenumber at

$\sim$475 cm^{-1} and decrease in intensity as the ZnO content increase. The intensity of the band at $\sim$533 cm^{-1} decreases with the increase of the ZnO content. The intensity of the band at $\sim$602 cm^{-1} increases as the ZnO content increase up to 30 mol%. The intensity of the bands at $\sim$660 and 797 cm^{-1} show maximum for the sample with 5 mol% ZnO, and then decreases as the ZnO content increase up to 30 mol%. The structural changes observed by increasing ZnO content in the $0.5Er^{3+}/2.5Yb^{3+}$ co-doped ($40Bi_2O_3$–$20GeO_2$–$(30 - x)$PbO–xZnO–$10Na_2O$) glass system and evidenced by the FT-IR investigation suggest that the ZnO ions play a network modifier and network former in the glass system.

Figure 3 shows the temperature dependence of the dc conductivity of the $0.5Er^{3+}/2.5Yb^{3+}$ co-doped ($40Bi_2O_3$–$20GeO_2$–$(30 - x)$PbO–xZnO–$10Na_2O$ where $x = 0.0$, 5, 10, 15, 20, 25, and 30 mol%) glass system. The slope of the curves which gives the activation energy for conduction W. The linear relationship between the logarithm of dc conductivity [ln σ; σ is expressed in $(\Omega m)^{-1}$] and inverse of temperature with a negative slope indicates that the following well-known Arrhenius law is satisfied [21, 22]:

$$\sigma = \sigma_0 \exp\left(\frac{-W}{kT}\right) \tag{2}$$

where $\sigma_0 = \mu N$ is the pre-exponential factor, N is the amount of charge carriers, and μ their electrical mobility. The activation energy for conduction W is the average value of the heights of the potential energy barriers that the mobile ion must overcome in its jumps, K is Boltzmann constant, and T is the temperature measured in Kelvins. From Fig. 4, it is observed that the dc conductivity in present glass system increase with rise in temperature. Also the dc conductivity is found to decreases with increase in the concentration of ZnO. The activation energy (W) and the atomic intermediate distance (R) are listed in Table 1.

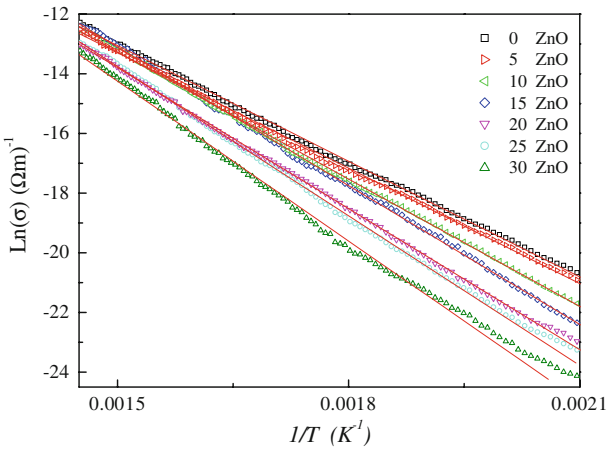

Fig. 3 Temperature dependence of dc conductivity (ln σ_{dc}) for different glass compositions

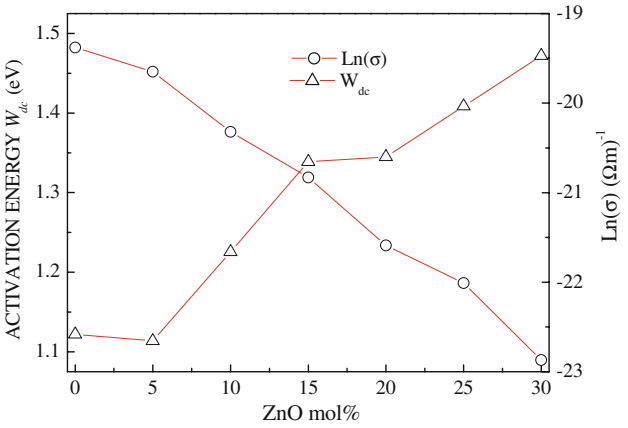

Fig. 4 Effect of ZnO content on dc conductivity (ln σ_{dc}) at $T = 476$ K and activation energy (W) for different glass compositions

In the range of measurements, W depends on the site-to-site distance R. These results show that there is a prominent positive correlation between W and R between the ions. This agrees with the results suggested by Sayer and Mansingh [23] and Salem [24] delineated the dependence of W on the atomic intermediate distance (R). The results in Table 1 indicate that as ZnO content increases, the atomic intermediate distance (R) increases. It is understood that this causes the activation energy for conduction W to increase, while causing the dc conductivity (σ) to decrease. On the other hand, the decrease in electrical conductivity of the glass system with the substitution of PbO by ZnO content can be attributed to the presence of Bi_2O_3 shows a blocking effect on the migration of mobile ions. Other authors considered similar arguments for the decrease in conductivity when in a binary glass; a third component was added [5]. Therefore, the conduction mechanism in the present glasses is purely ionic in nature and the mobile ions are sodium.

Figure 5 shows the transmittance and reflectance spectra of Er^{3+}/Yb^{3+} co-doped ($40Bi_2O_3$–$20GeO_2$–$(30 - x)$PbO–x ZnO–$10Na_2O$, where $x = 0, 5, 10, 15, 20, 25$, and 30 mol%) glass system. Each assignment in Fig. 6 corresponds to the absorptions from the ground state $^4I_{15/2}$ of Er^{3+} ions and $^2F_{7/2}$ of Yb^{3+} ions to the excited states. The absorption band of Yb^{3+} for the $^2F_{5/2} \rightarrow {}^2F_{7/22}$ transition overlaps that of Er^{3+} for the $^4I_{15/2} \rightarrow {}^4I_{11/2}$ transition. Compared with Er^{3+} ions, the absorption of Yb^{3+} near 980 nm is predominant. When the excitation was performed at the $^2F_{5/2}$ level with a diode laser of 975 nm, the emission from the $^2F_{5/2}$ state of Yb^{3+} overlaps the absorption band for the $^4I_{15/2}$–$^4I_{11/2}$ transition of Er^{3+} due to only one electronic excited state for Yb^{3+} ions. The energy transfer (ET) from Yb^{3+} to Er^{3+}, $^2F_{5/2}$ $(Yb^{3+}) + {}^4I_{15/2}(Er^{3+}) - {}^2F_{7/2}(Yb^{3+}) + {}^4I_{11/2}$ (Er^{3+}), acts as indirect pumping of Er^{3+}. So the ET efficiency will play an important role in Er^{3+}/Yb^{3+} co-doped system.

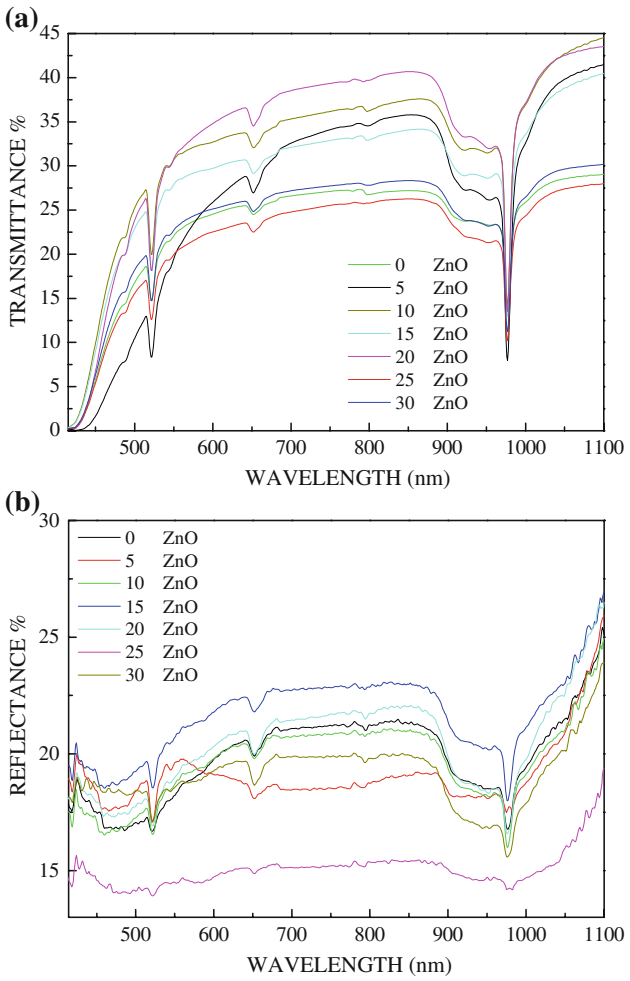

Fig. 5 The transmittance and reflectance spectra for different glass composition

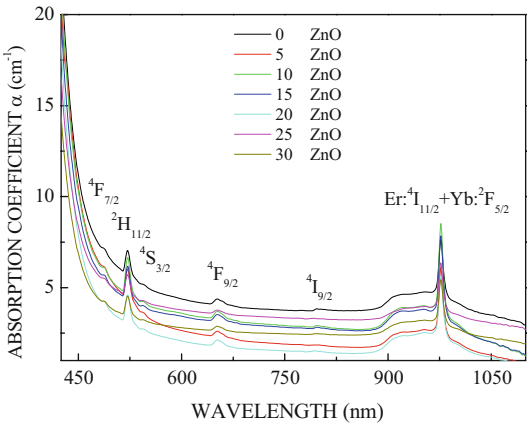

Fig. 6 The absorption coefficient as a function of wavelength for the glass system

Depending on the composition, the fundamental absorption edge is observed in the range of (414–434 nm). The optical absorption coefficient, α, which is the relative rate of decrease in light intensity along its path of propagation, was calculated from the transmittance and reflectance data in the wavelength range 190–1100 nm. Figure 6 shows a plot of α as a function of phonon energy for the glass system. The optical absorption coefficient α of samples which can be evaluated from the optical transmittance, reflectance, and the thickness of the sample (d) according to

$$\alpha = \frac{1}{d}\ln\frac{(1-R)}{T} \tag{3}$$

The absorption coefficient $\alpha(v)$ as a function of the photon energy (hv) for direct and indirect optical transitions, according to Pankove [25] is given by

$$\alpha(v) = \alpha_0\left(hv - E_{\text{opt}}\right)^P \Big/ hv \tag{4}$$

where α_0 is an energy-independent constant (band edge steepness parameter in Tauc's picture [26]). The exponent P determines the type of electronic transitions causing the absorption and takes the values 1/2, 3/2, 2, and 3 for direct allowed, direct forbidden, indirect allowed, and indirect forbidden transitions, respectively [26], i.e., power part $P = 2$; so, the values of indirect optical band-gap energy E_{opt} can be obtained from Eq. 4 by extrapolating the absorption coefficient to zero absorption in the $(\alpha hv)^P - hv$ plot as shown in Fig. 7. The respective values of E_{opt} are obtained by extrapolating to $(\alpha hv)^P = 0$, for direct allowed, direct forbidden, indirect allowed, and indirect forbidden transitions, respectively [26, 27]. Figure 7 shows the different values of P were applied to the present experimental data of the glass system. The energy of the optical band gap evaluated for the glass samples for ($P = 2$, 1/2, 3/2, and 3) are listed in Table 2. However, the experimental data give a better fit and reasonable values ($E_{\text{opt}} = 2.53$–2.62 eV), which are in good agreement with some reported values of related oxide glasses [27], for $P = 2$ which is corresponding to indirect allowed transitions. As seen in Table 2 the obtained values of the optical gap are changing according to the selected value of the exponent P. Moreover, the change in the value of the regression factor does not really decide which value of P is better to be selected. Therefore, Eq. 4 may be rather used only for the determination of the type of conduction mechanism, and the optical gap itself should be determined using another parameter, by which the exact value of exponent can be selected. The selected parameter is the imaginary part of the dielectric constant ε_2, which is a function of refractive index n and extinction coefficient k, and it will be discussed in detail next sections.

The optical absorption and particularly the absorption band edge is a good method for studying optically induced transition and gives information about the structure and

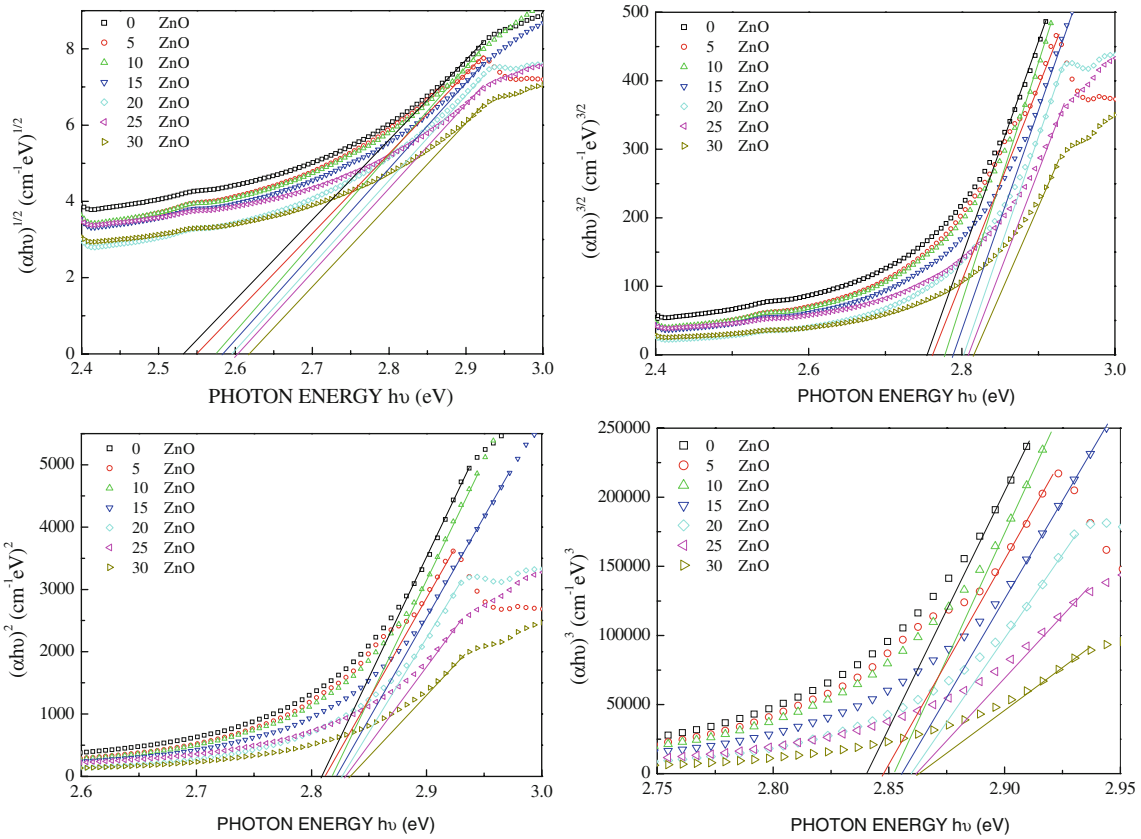

Fig. 7 The relation between photon energy eV and $(\alpha h\nu)^P$, where $P = 1/2$, 3/2, 2, and 3 for direct allowed, direct forbidden, indirect allowed and indirect forbidden transitions, respectively, for the glass system

Table 2 Optical energy gap values E_{opt} obtained for different types of electronic transitions $P = 1/2$, 3/2, 2, and 3 for direct allowed, direct forbidden, indirect allowed, and indirect forbidden transitions, respectively, and E_{opt} from ε_2 of Er^{3+}/Yb^{3+} co-doped $(40Bi_2O_3–20GeO_2–(30 - x)PbO–xZnO–10Na_2O$, where $x = 0$, 5, 10, 15, 20, 25, and 30 mol%) glasses

Glass no.	E_{opt} (eV)					E_r (eV)
	$P = 2$	$P = 1/2$	$P = 2/3$	$P = 1/3$	ε_2	
1	2.533	2.808	2.754	2.841	2.552	0.0059
2	2.542	2.811	2.762	2.847	2.595	0.0061
3	2.574	2.817	2.778	2.852	2.629	0.0058
4	2.583	2.821	2.788	2.855	2.645	0.0057
5	2.592	2.825	2.801	2.859	2.688	0.0058
6	2.601	2.829	2.809	2.862	2.699	0.0055
7	2.662	2.838	2.816	2.863	2.714	0.0051

optical energy gap in glasses. The absorption edge in many materials follows the Urbach rule [28].

$$\alpha(h\nu) = \alpha_o \exp\left(\frac{h\nu}{E_r}\right) \quad (5)$$

where α is the optical absorption coefficient, α_o is a constant and (E_r) is the energy width of the tail of localized state in the normally forbidden band gap. E_r is often interpreted as the width of the localized states in the band gap of the material. The exponential dependence of the optical absorption coefficient with photon energy may arise from the electronic transitions between the localized states, which have tailed odd in the band gap. The density of these states falls off exponentially with energy, which is consistent with the theory of Tauc [26]. However, the exponential dependence of the optical absorption coefficient on energy might arise from the random fluctuations of the internal fields associated with the structural disorder in

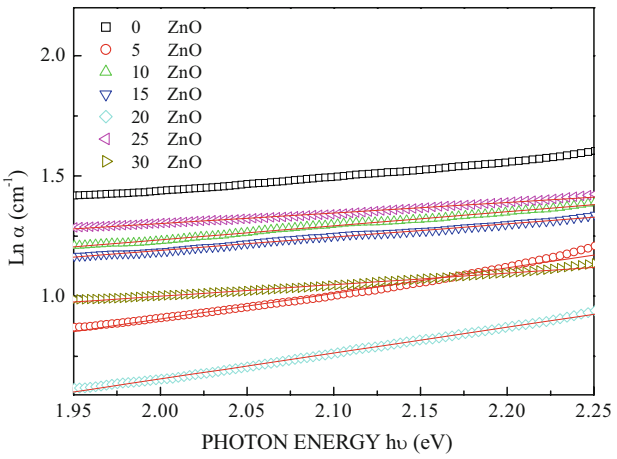

Fig. 8 The relation between ln α cm^{-1} and photon energy eV for the glass system

many materials. The width of the localized states (band tail energy or Urbach energy) E_r is estimated from the slopes of ln(α) vs. hv plots. Figure 8 shows the variation of ln α with incident photon energy hv for the glass system. As seen in the figure, the absorption edge is found to be exponentially dependent on the incident photon energy and obeys the empirical Urbach rule [28]. The width of the localized states E_r (band tail energy or Urbach energy) estimated from the slopes of ln α versus hv plots was found to be in the range 0.0051–0.0059 eV. A plot of E_{opt} for indirect allowed transition against ZnO content shows that E_{opt} increases with an increase in ZnO content as shown in Fig. 9. The increasing values of E_{opt} upon increasing the ZnO content can be understood in terms of the structural changes that are taking place in the studied glass system. According to the IR analysis, germanium and bismuth have more than one stable configuration [29, 30]; so, increasing of ZnO into such glass matrix at the expense of PbO, will weakness the glass network, by increasing the molar volume. Thus, the available oxygen environment around the

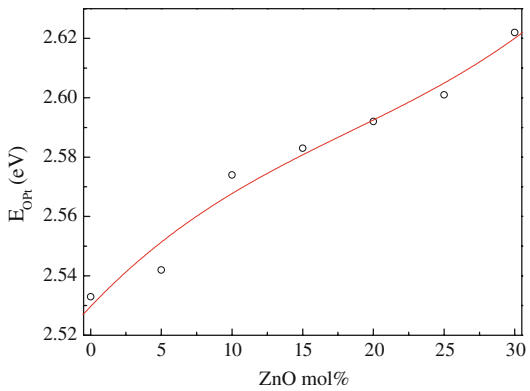

Fig. 9 The optical band gap E_{opt} as a function of ZnO content for the glass system

bismuth cations will decrease, and this will increase the values of E_{opt}.

A possible explanation of the general increase is a change in the structure of the glasses with increasing ZnO content. PbO in general is a glass modifier and enters the glass network by breaking up the bonds (normally the oxygens of PbO break the local symmetry, while Pb^{2+} ions occupy interstitial positions) and introduces coordinate defects known as dangling bonds along with non-bridging oxygen ions. However, PbO may also participate in the glass network with PbO_4 structural units when lead ion is linked to four oxygens in a covalency bond configuration [31]. Therefore, at high fractions of PbO, the content of pyramidal groups is high, resulting in a compacting of the network and a corresponding to the minimum value of the optical band gap for the sample free ZnO. On the other hand, ZnO [32] can act as network modifiers or as network formers. At low oxide content they act predominantly as network modifiers, but at higher contents network-forming groups of ZnO_4 are established [33]. Therefore, with increasing of ZnO at the expense of PbO content of pyramidal groups are decreased, resulting in reducing the compactness of the network and a corresponding increase of the optical band gap with the substitution of PbO by ZnO content.

According to the theory of reflectivity of light, the refractive index (n) as a function of the reflectance (R), and the extinction coefficient (k) are given by the quadratic equation

$$R = \frac{(1-n)^2 + K^2}{(1+n)^2 + K^2} \tag{6}$$

Figure 10a shows the refractive index n as a function of wavelength for the glass system. It is seen that the values of the refractive index n decreases as the wavelength increases. From the calculated refractive indices n and also based on the average molecular weights (M) of each glass samples. It is clear from the curves that the general behavior of n is the same for all samples at high frequencies. This can be explained by the fact that the hole exchange in the samples cannot follow the frequency [34]. The behavior of ε_2 and n suggests that the hole exchanges are in the local displacements of electrons or holes in the direction of the electric field, which then cause polarization. Figure 10b shows a plot of the extinction coefficient k, for the glass system, which is calculated according to the following relation

$$k = \alpha\lambda/4\pi \tag{7}$$

Figure 11 shows the fundamental absorption band which could be determined from the measurements of reflectivity at normal incidence [26]. The absorption band is obtained when the imaginary part of the dielectric constant is plotted

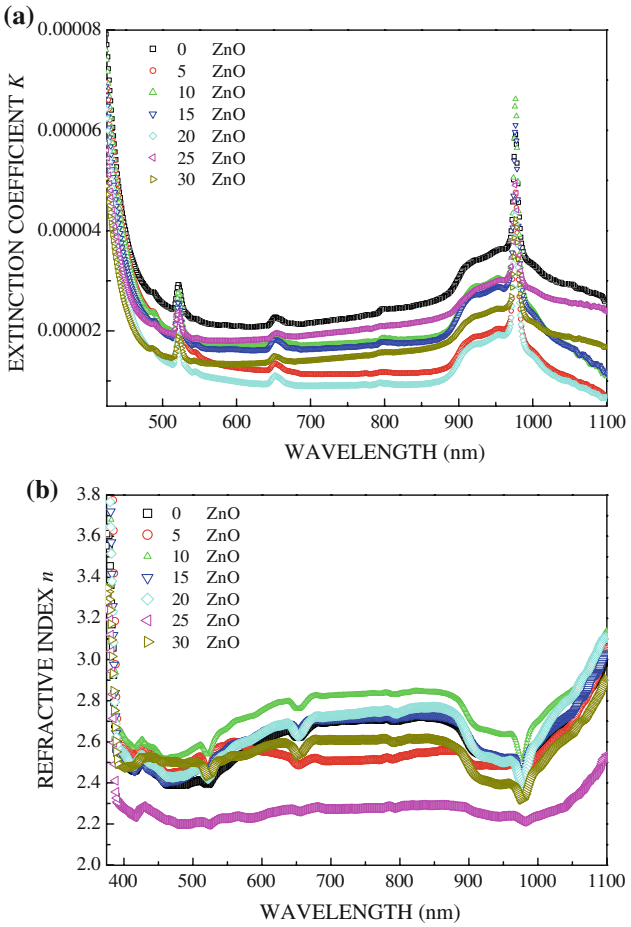

Fig. 10 **a** The extinction coefficient k and **b** refractive index n as a function of wavelength for the glass system

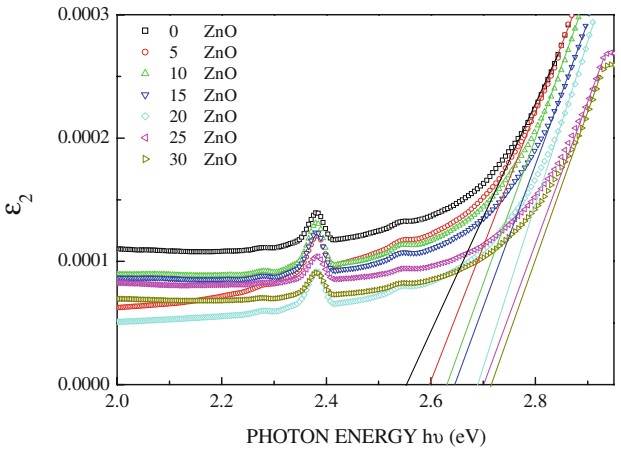

Fig. 11 The imaginary part of the dielectric constant is plotted as a function of photon energy for the glass system

as a function of photon energy. Dielectric constant is connected to the refractive index according to

$$(n+ik)^2 = \frac{\varepsilon}{\varepsilon_o} = \frac{\varepsilon_1 + \varepsilon_2}{\varepsilon_o} \tag{8}$$

Separation of the real part and the imaginary parts, leads to the real and imaginary parts:

$$\varepsilon_1 = n^2 - k^2 \quad \text{and} \quad \varepsilon_2 = 2nk \tag{9}$$

Galeener and Lucovsky [35] studied infrared-active vibrational modes in glasses and showed that peaks in the spectrum are associated with vibrations ε_2 having transverse-optical-mode character. However, zero crossings of occur at longitudinal optical ε_1 phonon frequencies. Therefore, spectrum ε_2 should reflect the vibrational character of the glass samples. On a comparison of the optical energy gap values obtained from the transmittance and reflectance spectra in the case of indirect allowed transition ($E_{opt} = 2.53$–2.62 eV) which are in good agreement with the values estimated from the dielectric measurements ε_2 ($E_{opt} = 2.55$–2.71 eV), however, the type of electronic transitions in the present glass system is indirect allowed.

Conclusions

From the present study, it is observed that the density decreases with increase in ZnO content due to the replacement of heavy metal oxides PbO by lighter ZnO. The infrared spectral analysis of the present glass system shows that Bi^{3+} cations are incorporated in the glass network as [BiO_3] pyramidal and [BiO_6] octahedral units. The band at 533 cm^{-1} is due to vibrations of Bi–O bonds in the [BiO_6] polyhedra, while the shoulder at 832 cm^{-1} is related to symmetrical stretching vibrations of the Bi–O bonds in the [BiO_3] groups. The band from $\sim$832 cm^{-1} disappears and a new band situated at $\sim$875 cm^{-1} is present in the samples containing 15, 20, 25, and 30 mol%. This suggests the conversion of the BiO_3 into BiO_6 structural units with the increasing of ZnO content in the glass samples. The presence of IR band in the range 400–600 cm^{-1} indicates the presence of Zn–O tetrahedral bending vibrations in the present glass system. The dc conductivity decreases and activation energy increases with increase in ZnO content. The activation energy W and the atomic intermediate distance R are increases with increase in ZnO content. The electrical conduction in present glass system is purely ionic in nature. The optical band gap increases with increase in ZnO content due to the decrease in the available oxygen environment around the bismuth cations. Both the optical gap E_{opt} and the band tail E_r behave oppositely. The optical energy gap obtained from the transmittance and reflectance spectra in the case of indirect allowed transition $E_{opt} = 2.53$–2.62 eV which are in good agreement with the estimated values from the dielectric measurements $E_{opt} = 2.55$–2.71 eV. Therefore, the type of electronic transitions in the present glass system

is indirect allowed, and the present glasses behave as indirect gap semiconductors.

References

1. Bale S, Rahman S, Awasthi AM, Sathe V (2008) J Alloys Compd 460:699
2. Rani S, Sanghi S, Anshu, Agarwal A, Kishore N, Seth VP (2008) J Phys Chem Solids 69:1855
3. Ganguli M, Rao KJ (1999) J Solid State Chem 145:65
4. Dumbaugh WH (1986) Phys Chem Glasses 27:119
5. Sindhu S, Sanghi S, Agarwal A, Seth VP, Kishore N (2005) J Mater Chem Phys 90:83
6. Lakshminarayana G, Buddhudu S (2005) Spectrochim Acta A 62:364
7. Xu S, Yang Z, Zhang J, Wang G, Dai S, Hu L, Jiang Z (2004) Chem Phys Lett 385:263
8. Hutchinson JA, Allik TH (1992) Appl Phys Lett 60(12):1424
9. Balda R, Fernández J, Arriandiaga MA, Fdez-Navarro JM (2004) Opt Mater 25(2):157
10. Pascuta P, Pop L, Rada S, Bosca M, Culea E (2008) J Vib Spectrosc 48:281
11. Motke SG, Yawale SP, Yawale SS (2002) Bull Mater Sci 25(1):75
12. Bale S, Rahman S (2008) J Opt Mater 31:333
13. Baia L, Iliescu T, Simon S, Kiefer W (2001) J Mol Struct 259:9
14. Céreyon A, Champagnon B, Martinez V, Maksimov L, Yanush O, Bogdanov VN (2006) Opt Mater 28:1301
15. Kassab LRP, Hora WG, Martinelli JR, Sene FF, Jakutis J, Wetter NU (2006) J Non-Cryst 352:3530
16. Knoblochova K, Ticha H, Schwarz J, Tichy L (2009) J Opt Mater 31:895
17. Simon S, Todea M (2006) J Non-Cryst Solids 352:2947
18. Pan Z, Morgan SH, Loper A, King V, Long BH, Collins WE (1995) J Appl Phys 77(9):4688
19. Huang K (1981) Contemp Phys 22:599
20. Layne CB, Lowdermilk WH, Weber MJ (1977) Phys Rev B 16:10
21. Mott NF, Davis EA (1979) Electronic processes in non-crystalline materials, 2nd edn. Clarendon Press, Oxford
22. Mott NF (1974) Metal insulator transitions. Taylor & Francis, London
23. Sayer M, Manshingh A (1972) Phys Rev B 6:4629
24. Salem SM (2009) J Mater Sci 44:5760. doi:10.1007/s10853-009-3807-y
25. Pankove J (1971) Optical processes in semiconductors. Prentice-Hall, Englewood Cliffs
26. Tauc J (1974) Amorphous and liquid semiconductor. Plenum, New York
27. Lakshminarayana G, Buddhudu S (2006) J Spectrochim Acta A 63:295
28. Urbach F (1953) Phys Rev 92:1324
29. Yiannopoulos Y, Chryssikos G, Kamitsos E (2001) Phys Chem Glasses 42:164
30. El-Egili K, Doweidar H (1998) Phys Chem Glasses 39:332
31. Raghavaiah BV, Laxmi Kanth C, Krishna Rao D, Lakshman Rao J, Veeraiah N (2005) J Mater Lett 59:539
32. Scholze H (1991) Glass nature, structure and properties. Springer, New York
33. Doweidar H, El-Damrawi G, Moustafa YM, Hassan AK (1999) Phys Chem Glasses 40(5):252
34. Soliman Selim M, Turky G, Shouman MA, El-Shobaky GA (1999) Solid State Ionics 120:173
35. Galeener FL, Lucovsky G (1976) Phys Rev Lett 37:1474